

Review of Selected Multi-Element Resonant Topologies

Juraj Koscelnik¹⁾, Roman Mazgut¹⁾, Slavomir Kascak¹⁾ and Michal Prazenica¹⁾

¹⁾ Department of Mechatronics and Electronics, Zilina, Slovakia, e-mail: prazenica@fel.uniza.sk

Abstract — The paper deals with an analysis and comparison of multi-element resonant topologies. The superior performance of the investigated converters provides inherent current protection and very low circulating energy. The converter consists of two resonant tanks and HF transformer in case of the LCTL topology. The paper shows the design of the resonant elements. The converters can achieve zero current switching (ZCS) and zero voltage switching (ZVS) conditions for the primary and secondary-side of the device respectively. The converters achieve high values of power density and efficiency up to 96 % at the full load. The paper includes the basic equations, analysis and simulation of the chosen topologies (LCTL, LCLCL, LCL2C2).

Keywords — Multi-element resonant converter, review of the resonant converters, switching conditions, LCTL, LCLCL, LCL2C2.

I. INTRODUCTION

The progress in the development of semiconductor devices has resulted in formation of a new field of science generally called power electronics (Fig. 1). The newer and higher quality parts affect design of the resonant converter and therefore it is necessary to use sophisticated control algorithms.

In some involvement inverters with high frequency transformers the number of the semiconductor devices in converter may be reduced and this results in price of the product [1]–[3]. Increasing functionality requires more power consumption and higher density requires less size of the power supplies. Therefore, the power supplies for computing, consumer electronics and lighting applications are required to provide more power with small size and low cost.

The most effective way to achieve high power density in converters is to increase the switching frequency so that the size of the passive components, such as the capacitor and inductor, as well as the transformer can be reduced, as they occupy a large portion of the overall size [1].

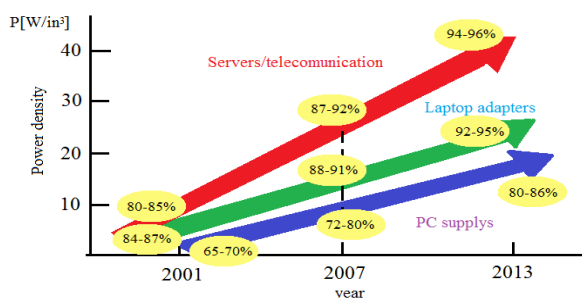


Fig. 1. Course of the power density development.

II. RESONANT CONVERTERS

The group of resonant and quasi-resonant converters consists of series, parallel and series-parallel resonant circuits. By combining the basic resonant circuits modified multi-element resonant circuits arise. Resonant converters use two kinds of the switching technique: Zero voltage switching (ZVS) and Zero current switching (ZCS) [3]. Those techniques are known as soft switching. The converter can operate in ZVS and/or ZCS. The basic diagram of the resonant converter is in Fig. 2.

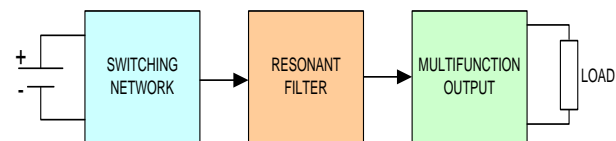


Fig. 2. Diagram of the resonant converter.

The diagram describes basic connection of the resonant converter composed of the DC source; switching network; resonant filter and multifunction output connected to a load.

A. Multi-resonant Converters

The essence of the multi-resonant switch concept is to combine the desirable characteristics of both quasi-resonant switches in one device. This can be achieved using the multi-resonant switch. In this configuration of the resonant switch, resonant capacitances are placed in parallel with both the switch and the diode, resulting in desirable zero-voltage switching of both devices Zero-Voltage-Switched Multi-Resonant Converters (ZVS-MRCs) generated from PWM topologies by replacing the PWM switch by the multi-resonant switch [2]. The multi-resonant network absorbs all major parasitic components, including the transistor output capacitance, diode junction capacitance and transformer leakage inductances into the resonant circuit. This allows the multi-resonant converters to operate at high frequencies with the most favourable (zero-voltage) switching condition for all semiconductor devices [4], [5]. The base of every multi-element resonant converter is that it is usually composed of five resonant components in series or parallel circuit connection. This connection forms the resonant tank.

Using a similar concept, a family of multi-element resonant converters is proposed. Some of the five-element resonant tanks are shown in Fig. 3. Due to space limitations, the formation of all five-element resonant converters cannot be exhibited completely in this work.

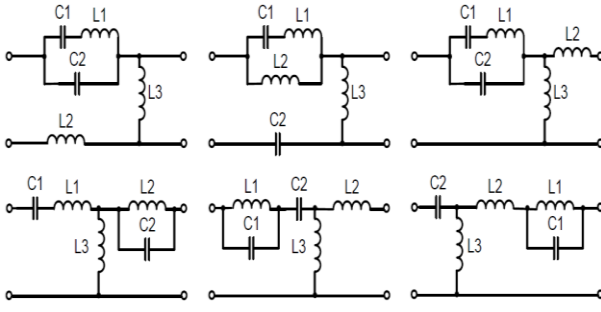


Fig. 3. Possibilities of the multi-element connections of the resonant converters.

III. COMPARISON OF SELECTED MULTI-ELEMENT TOPOLOGIES

As it is described in the previous chapter the multi-element resonant converter is composed of five accumulation elements. There are many possibilities of circuit connections. For this chapter three topologies were chosen: CTLCL, LCLCL and LCL2C2. For the review it was done the simulation analysis provided by the MATLAB and OrCAD software.

A. LCTLCL Topology

LCLCL converters (Fig. 4) are one of the novel types of converters based on the LLC resonant circuit, and LCTLCL inverter consisting of the DC/DC buck converter LCLC resonant filter and HF transformer. The HF transformer can also be connected behind the LCLC filter, if necessary and it can also be used to the DC/DC boost converter types. The inverter (LCTLCL) is usually used as a power supply for either HV rectifiers or HF cycloconverters or matrix converters for 2-phase motor applications respectively [6], [7].

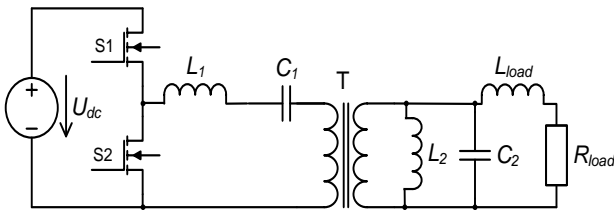


Fig. 4. Basic diagram of the LCTLCL inverter.

The resonant converter is composed of one series resonant tank (L_1, C_1), HF transformer (T) and parallel resonant tank (L_2, C_2). The converter is fed by a DC source and the shape of the input voltage is switched by two switches (S1, S2) in half-bridge connections [7]. In this case the output of the filter is the HF harmonic waveform of the voltage (and current) – direct AC output mode with THD not more than 5 %.

For the analysis, an equivalent LCTLCL circuit can be created. The equivalent parameters of the HF transformer ($L_\sigma, R_\sigma, L_m, R_{Fe}$) and inter-winding capacitance C_{iw} and inter-turn capacitance C_{it} are included into the resulting component parameters. More about the equivalent circuit is given in the paper [7]. On the basis of it the state-space equations for the equivalent circuit with the R-L load will be [6]:

$$\frac{di_{L1}}{dt} = \frac{1}{L_1} u(t) - \frac{R_1}{L_1} i_{L1} - \frac{1}{L_1} u_{C1} - \frac{1}{L_1} u_{C2} \quad (1)$$

$$\frac{di_{L2}}{dt} = \frac{1}{L_2} u_{C2} \quad (2)$$

$$\frac{du_{C1}}{dt} = \frac{1}{C_1} i_{L1} \quad (3)$$

$$\frac{du_{C2}}{dt} = \frac{1}{C_2} i_{L1} - \frac{1}{C_2} i_{L2} - \frac{1}{C_2 R_2} u_{C2} - \frac{1}{C_2} i_{Ll} \quad (4)$$

$$\frac{di_{Ll}}{dt} = \frac{1}{L_{load}} u_{C2} - \frac{R_{load}}{L_{load}} i_{Ll} \quad (5)$$

where i_{L1} , i_{L2} are currents in the inductors L_1 and L_2 , respectively; i_{Ll} is current in the load R_2, L_2 ; u_{C1}, u_{C2} are capacitor voltages of C_1 and C_2 , respectively, $u(t)$ is the output voltage of the converter (filter input voltage). When the input voltage U_{DC} is varying than the RMS value of the fundamental harmonic will also vary. To be constant an asymmetric control of the duty cycle for the switches S_1, S_2 has to be provided [7], [8].

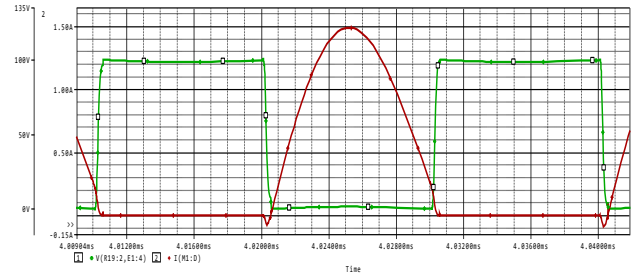


Fig. 5. Switching waveforms of the transistor (current I_D – red line, voltage U_{DS} – green line).

Fig. 5 shows voltage and current of the MOSFET transistor. It is also visible that the transistor is turning on in the zero voltage, the conditions preferred for the MOSFET transistors. The output voltage and current of the resonant converters is quasi harmonic. Simulation results of the LCTLCL converter confirm the theoretical assumptions. Following figure shows the output waveforms of the proposed resonant converter.

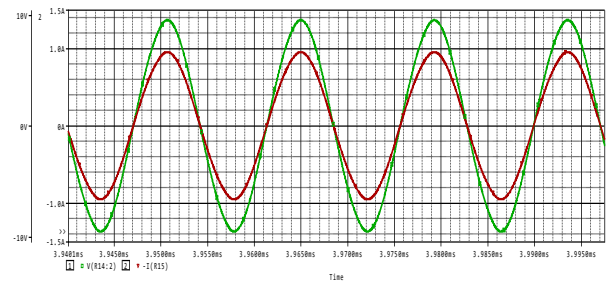


Fig. 6. Output waveforms of the LCTLCL resonant converter (current I_L – red line, voltage U_L – green line).

Fig. 6 shows the output voltage and current in the steady state. The phase shift was 0° el. due to purely resistant load. The simulated THD value of the output voltage was 4.9 % what met converter requirements.

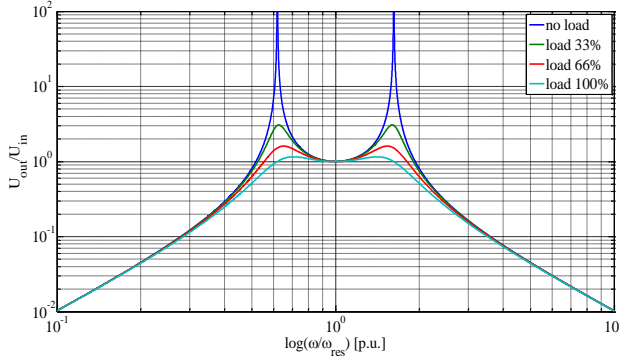


Fig. 7. Voltage transfer function U_2/U_1 of the LCTL filter (Bode diagram).

The voltage transfer function shows that if switching frequency is equal to the resonant frequency the voltage gain is equal 1. Also, in this point the LCTL converter is not depending on the load magnitude (Fig. 7).

B. LCLCL Topology

The proposed multi-element resonant converter is implemented and illustrated in Fig. 8. The LCLCL resonant tank is selected as the core of this converter. The half-bridge topology is adopted as the primary-side structure. It is easy to extend it to other types of input structures, including full-bridge, stacked half-bridge, and three-level structures. The centre type structure with synchronous rectifiers (SR) is chosen for use on the secondary side. Similarly, it is easy to use other types of output structures, such as the full-bridge, voltage-doubler and current-doubler structures. The secondary side with the SR is better for the low-voltage output applications. The secondary-side devices can be replaced by diodes for high-voltage applications. Thus, complicated SR driving circuits can be avoided. For the front-end converters, the SR output is applied to increase the efficiency [9].

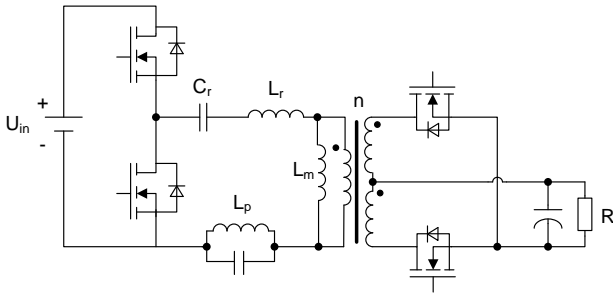


Fig. 8. Diagram of the LCLCL resonant converter with the SR.

This topology is well known and well described in the scientific literature. The resonant circuit is composed of series-parallel LLC circuit and one parallel circuit. With one additional resonant element, a second band pass filter is created. A novel LCLCL resonant tank is proposed as an example. The basic resonant tank cell is shown in Fig. 8. The structure is similar to the previously proposed four element resonant tank, but an extra resonant inductor is inserted.

The voltage gain of the proposed LCLCL resonant tank is illustrated in Fig. 9. The curves in Fig. 9 are dependent on the load (10–100 % load).

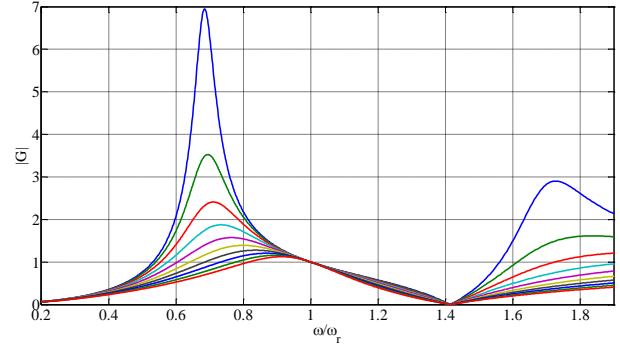


Fig. 9. Voltage transfer function U_2/U_1 of the LCLCL filter.

Conceptually, L_r , C_r and L_p contribute to the first band pass filter at low frequencies. The second band pass filter consists of L_r , C_r and C_p , which dominate at high frequencies. The first band pass filter can help to deliver the fundamental component to the load. It functions as the traditional resonant converters. The second band pass filter enhances the power delivery with utilization of higher harmonics. Consequently, with the injection of higher-order harmonics, the reactive power of the resonant tank can be reduced and lower RMS current and lower conduction loss can be achieved.

$$f_{01} \approx \frac{1}{2\pi} \sqrt{(L_r + L_p)C_r} \quad (6)$$

$$f_{02} = \frac{1}{2\pi} \frac{1}{\sqrt{L_p C_p}} \quad (7)$$

$$f_{03} \approx \frac{1}{2\pi} \sqrt{L_r \frac{C_r C_p}{C_r + C_p}} \quad (8)$$

$$f_{04} = \frac{1}{2\pi} \frac{1}{\sqrt{C_r(L_r + L_m + L_p)}} \quad (9)$$

$$Z_0 = L_r 2\pi f_{01} \quad (10)$$

For the MOSFETs, the ZVS operation is preferred. As a result, the LCLCL resonant converter can perform boost or buck functioning, according to what is required. For the front-end converters, higher voltage gain is necessary during the holdup time. Therefore, the ZVS Region II is favorable during the holdup time operation. For overload, startup and short output conditions, the ZVS Region I is preferred to limit the current [7].

At the nominal condition, the LCLCL resonant converter operates at the resonant frequency f_{01} , where nearly ZV-ZCS condition can be achieved for the primary-side devices. The current of the secondary-side rectifiers naturally falls to zero, and the reverse recovery issue is eliminated [1], [4]. The topology works with 3rd harmonic as well and uses its injection to the output voltage to increase its RMS value ($0.9 U_m$) [7].

C. LCL2C2 Topology

In case of demand of a harmonic sinusoidal voltage for the critical load, it is necessary to use some of the resonant filter types. The resonant components are tuned to the basic harmonic. The LCL2C2 filter can be supplied by

either single-phase voltage inverter in the full- or half-bridge connection. A diagram of the resonant converter is shown in Fig. 10.

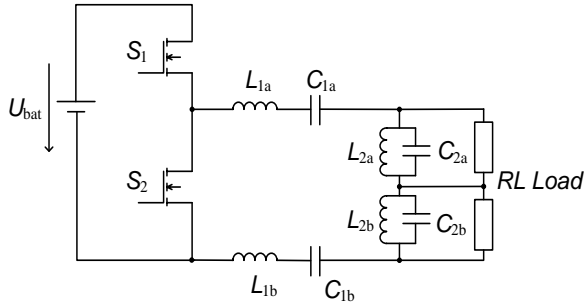


Fig. 10. Diagram of the LCL2C2 converter.

The converter in Fig. 10 can be classified as the DC/AC converter with the resonant filter. On the contrary, the following analysis is oriented on the design analysis of the LCLC components, investigation of the transfer- and transient properties and on influence of non-linearity of the inductors [10].

The state space model equations of the LCL2C2 converter are:

$$\frac{di_{L1a,b}}{dt} = -\frac{r_1}{L_1} i_{L1} - \frac{1}{L_1} u_{C2a} - \frac{1}{L_1} u_{C2b} + \frac{1}{L_1} u(t) \quad (11)$$

$$\frac{du_{C1a,b}}{dt} = \frac{1}{C_1} i_{L1} \quad (12)$$

$$\frac{du_{C2a}}{dt} = \frac{1}{C_{2a}} i_{L1} - \frac{1}{C_{2a}} i_{L2a} - \left(\frac{1}{r_a} + \frac{1}{R_a} \right) \frac{1}{C_{2a}} u_{C2a} \quad (13)$$

$$\frac{du_{C2b}}{dt} = \frac{1}{C_{2b}} i_{L1} - \frac{1}{C_{2b}} i_{L2b} - \left(\frac{1}{r_a} + \frac{1}{R_a} \right) \frac{1}{C_{2b}} u_{C2b} \quad (14)$$

$$\frac{di_{L2a}}{dt} = \frac{1}{L_{2a}} u_{C2a} \quad (15)$$

$$\frac{di_{L2b}}{dt} = \frac{1}{L_{2b}} u_{C2b} \quad (16)$$

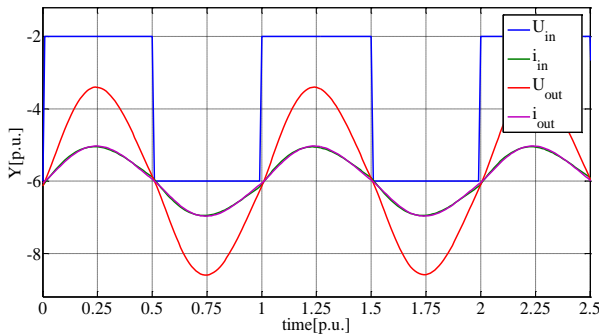


Fig. 11. Simulated waveforms of the LCL2C2 inverter (p.u.).

Fig. 11 shows simulated waveforms of the proposed resonant converter. The output current and voltage have a quasi-harmonic shape with the THD up to 5 %. The input voltage has a value from zero up to maximum value of the voltage what is due to the half-bridge connection of the switching network.

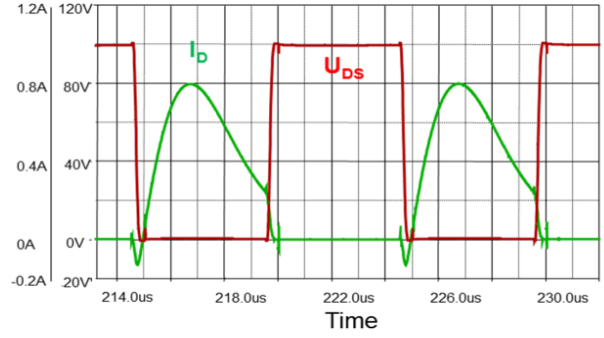


Fig. 12. Switching curves of the voltage and current of the MOSFET transistor.

The OrCAD analysis in Fig. 12 shows the waveform of the transistor. As it can be seen, the LCL2C2 converter works in the ZVS region. This region is preferred for the MOSFET transistors. The resonant frequency is set higher than switching frequency to operate in the ZVS region [11], [12].

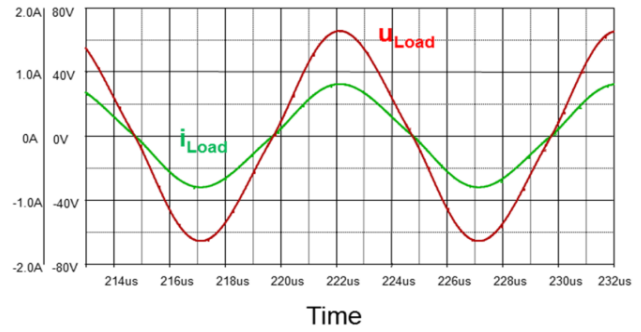


Fig. 13. Output voltage and current of the LCL2C2.

The output voltage and current have quasi harmonic shape (Fig. 13). The phase shift is equal 0 °el. due to purely resistive load. To achieve it in reality it is almost impossible due to parasitic components. The analysis confirms the theoretical assumptions for the LCL2C2 resonant converter. Using the FFT, measured THD of the output voltage of the proposed converter was 4.589 %. It is also clear that only the fundamental harmonic is at the output and a small value of the 3th and all other harmonics are suppressed [8], [9].

IV. EXPERIMENTAL VERIFICATION

The experimental measurements have been done on the physical sample (Fig. 14)

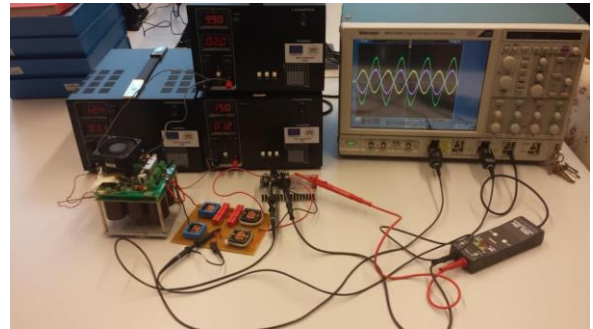


Fig. 14. Experimental set-up for the LCL2C2 converter.

The resonant converter was designed to operate in the ZVS region. This confirms the switching waveforms of

the semiconductor transistor given in Fig. 15. The ZVS is in the required operation area for the MOSFET transistor in order to reduce losses.

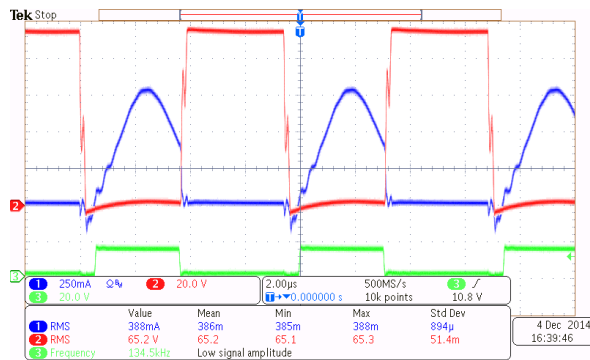


Fig. 15. Switching waveforms of the transistor.

The waveforms in Fig. 16 are showing the output voltage and voltage on both branches with a symmetric output of the LCL2C2 circuit. The load voltage (also voltage on the branches) has harmonic shape with low THD value in both legs.

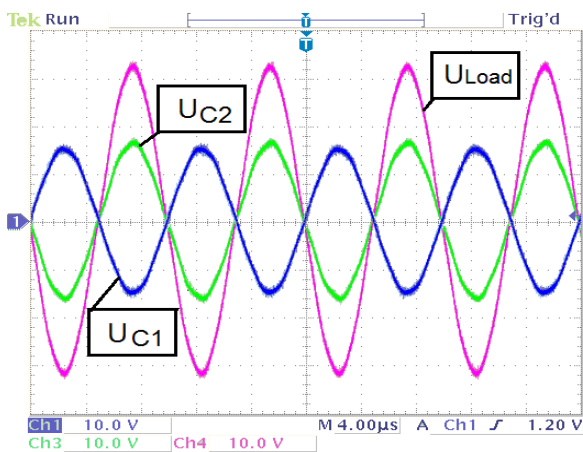


Fig. 16. Measured symmetrical output of the LCL2C2 circuit.

Parameters:

$U_{in} = 100 \text{ V}$, $f_{sw} = 100 \text{ kHz}$, MOSFETs = IRF5N50C, L_{1a} , $L_{1b} = 66 \text{ μH}$, L_{2a} , $L_{2b} = 66 \text{ μH}$, C_{1a} , $C_{1b} = 39 \text{ nF}$, C_{2a} , $C_{2b} = 39 \text{ nF}$, load: $R_{1,2}$, $L_{1,2} = 42 \text{ Ohm}$, 20 nH of parasitic inductance.

V. CONCLUSION

In the paper it is presented the review of the multi-element resonant converters. Chapter III describes selected topologies and simulation analysis. For the simulation the MATLAB and OrCAD software was used.

The LCTLCL belongs to new multi-element topologies. The connection reaches high values of the power density, efficiency up to 94 % and THD < 5 % which meets requirements for an equipment. Voltage transfer functions show that in the point where value of the switching frequency is equal to the resonant frequency the voltage gain is equal 1. Under these conditions the converter does not depend on the magnitude of the load.

The LCLCL is generally known topology. In the area of the resonant frequency No. 3 (f_{03}) where the voltage gain is equal to zero the converter short-circuit is proof. The topology works with 3th harmonic and uses its injection to the output voltage to increase its RMS value ($0.9 U_m$).

The LCL2C2 is new and still not deeply investigated topology. The connection brings possibility of multifunctional output – DC, AC with HF or LF. Essences of the topology are two parallel resonant circuits which can replace center tapped transformers. Therefore, it is possible as a 2nd stage of the converter utilized half-bridge circuit connection, what decreases the number of the semiconductor devices. The LCL2C2 topology is short-circuiting proof as well. Therefore, the LCL2C2 was connected without transformer and the converter can reach efficiency up to 97 %. The THD value is above 4.5 % and power density up to 93 W/in³.

ACKNOWLEDGMENT

The authors wish to thank for the financial support to the APVV 0314/12 and R&D operational program Centre of excellence of power electronics systems and materials for their components No. OPVaV-2008/2.1/01-SORO, ITMS 26220120046 funded by the European regional development fund (ERDF).

REFERENCES

- [1] W.A. Tabisz, F.C.Y. Lee: Zero-voltage-switching Multiresonant Technique-a Novel Approach to Improve Performance of High-frequency Quasi-resonant Converters, *Power Electronics*, IEEE Transactions, vol.4, No.4, pp.450-458, Oct 1989.
- [2] D. Fu: Topology Investigation and System Optimization of Resonant Converters, PhD. thesis, February 4, 2010, Blacksburg : Virginia
- [3] M. Frivaldsky, P. Drgona, P. Spanik: Experimental Analysis and Optimization of Key Parameters of ZVS Mode and its Application in the Proposed LLC Converter Designed for Distributed Power System Application, *Intern. J. of Electrical Power & Energy Systems*, vol. 47, pp. 448-456, May 2013
- [4] J. Dudrik, N. D. Trip, Soft-Switching PS-PWM DC-DC Converter for Full-load Range Applications, *IEEE Transactions on Industrial Electronics*, vol. 57, No. 8, 2010, pp. 2807-2814m, ISSN 0278-0046.
- [5] S. Kascak, J. Sedlak, Synthesis of LCLC Type Power Resonant Filter with Integrated Transformer, *University of Zilina : Faculty of Electrical Engineering*, 2010
- [6] Luo, F.L., Ye. H.: Energy Factor and Mathematical Modeling for Power DC/DC Converters, *IEE Proc. on Electrical Power Application*, vol. 152, p. 191-198
- [7] B. Dobrucky, M. Benova, S. Kascak, Transient Analysis and Modelling of 2nd- and 4th-Order LCLC Filter under Non-symmetrical Control, *Electronics and Electrical Engineering*, No.5(111), 2011, ISSN 1392-1215.
- [8] M. Ocilka, D. Kovac, I. Kovacova, J. Perdulk, A. Gladyr, D. Mamchur, I. Zachepa, T. Vince, J. Molnar, Serial Resonant Converter and Load Coll for High Frequency Heating, *Communications - Scientific Letters of University of Zilina*, vol. 15, No. 3, 2013, ISSN 1335-4205
- [9] J. Dudrik, P. Spanik, N. D. Trip, Zero Voltage and Zero Current Switching Full-Bridge DC-DC Converter with Auxiliary Transformer, *IEEE Transactions on Power Electronics*, ISSN 0885-8993, vol. 21, No. 5, September 2006, pp. 1328-1335
- [10] M. Youssef, "Analysis and Design of LCC Resonant Inverter for the Transportation Systems Applications", *Applied Power Electronics Conference and Exposition (APEC)*, 2010 Twenty-Fifth Annual IEEE, 2010, ISBN 978-1-4244-4783-1.
- [11] Zhong Ye, "Dual Half-Bridge DC/DC Converter with Wide-Range ZVS and Zero Circulating Current ", *Proc. of IEEE-ECCE'09 Int'l Conf.*, 2009, pp. 1353-1361, ISBN 978-1-4244-2893-9.
- [12] Y.A Ang, M.P. Foster, C.M Bingham, D.A. Stone, H.I. Sewell and D. Howe, (2004), "Design oriented analysis of fourth-order LCLC converters with capacitive output filter," *Electric Power Applications*, IEE Proceedings -, vol.152, no.2, pp.310,322, 4 March 2005